Observations of Active Region Loops with the EUV Imaging Spectrometer on Hinode

Harry P. Warren[1], Ignacio Ugarte-Urra[1,2], George A. Doschek[1], David H. Brooks[1,2], and David R. Williams[3]

ABSTRACT

Previous solar observations have shown that coronal loops near 1 MK are difficult to reconcile with simple heating models. These loops have lifetimes that are long relative to a radiative cooling time, suggesting quasi-steady heating. The electron densities in these loops, however, are too high to be consistent with thermodynamic equilibrium. Models proposed to explain these properties generally rely on the existence of smaller scale filaments within the loop that are in various stages of heating and cooling. Such a framework implies that there should be a distribution of temperatures within a coronal loop. In this paper we analyze new observations from the EUV Imaging Spectrometer (EIS) on *Hinode*. EIS is capable of observing active regions over a wide range of temperatures (Fe VIII–Fe XVII) at relatively high spatial resolution (1″). We find that most isolated coronal loops that are bright in Fe XII generally have very narrow temperature distributions ($\sigma_T \lesssim 3 \times 10^5$ K), but are not isothermal. We also derive volumetric filling factors in these loops of approximately 10%. Both results lend support to the filament models.

Subject headings: Sun: corona

1. Introduction

High spatial resolution solar observations have shown that coronal loops with temperatures near 1 MK have properties that are difficult to reconcile with physical models. Loops at

[1]Space Science Division, Naval Research Laboratory, Washington, DC 20375

[2]College of Science, George Mason University, 4400 University Drive, Fairfax, VA 22030

[3]Mullard Space Science Laboratory, University College London, Holmbury St Mary, Dorking, Surrey, RH5 6NT

these temperatures persist for much longer than a radiative cooling time, suggesting quasi-steady heating. The densities inferred from the observations, however, are much higher than can be reproduced by steady, uniform heating models. The temperature gradients along the loops are also much smaller than predicted by the simple models. (e.g., Lenz et al. 1999; Aschwanden et al. 2000; Winebarger et al. 2003).

Several models have been proposed to explain the properties of coronal loops at these temperatures. Aschwanden et al. (2000), for example, suggested that the observed loops were actually composed of smaller scale threads that were steadily heated at their footpoints. Footpoint heating leads to somewhat higher densities and flatter temperature gradients relative to steady heating models. At high densities, however, loops at these temperatures can become thermodynamically unstable (e.g., Mok et al. 2005; Müller et al. 2004; Winebarger et al. 2003), leading to catastrophic cooling. Multi-thread, impulsive heating models have also been suggested (e.g., Warren et al. 2003). In these models the fact that loops cool much more rapidly than they drain accounts for the high densities. Multiple threads in various stages of heating and cooling are needed to explain the observed lifetimes and temperature gradients. In both cases, these multi-thread models indicate the need for emission formed over a range of temperatures to reproduce the observed intensities (see also Reale & Peres 2000).

One limitation of the observational results from *TRACE* is that they are derived from narrowband filtergrams with somewhat limited diagnostic capabilities. The launch of the EUV Imaging Spectrometer (EIS) on the *Hinode* mission provides us with an opportunity to revisit some of these observational results using spectroscopic data. EIS is a high spatial and spectral resolution spectrometer that covers much of the same wavelength range as *TRACE*. EIS has a very broad temperature coverage and can image the solar corona in individual emission lines from the lower transition region to the hottest flares.

In this paper we focus on measuring the emission measure distribution in coronal loops near 1 MK. We have selected 20 relatively isolated loop segments from several different active region observations and computed differential emission measure distributions from the background subtracted loop intensities. For this work we focus on loops that are bright in Fe XII and find that for these loops the distribution of temperatures is almost always narrow, with a dispersion of several times 10^5 K. We also find volumetric filling factors of approximately 10%. These results support the idea that coronal loops are composed of smaller scale filaments that are below the spatial resolution of current solar instruments.

2. Observations

The EIS instrument on *Hinode* produces high resolution stigmatic spectra in the wavelength ranges of 171–212 Å and 245–291 Å. The instrument has 1″ spatial pixels and 22.3 mÅ spectral pixels. Further details are given in Culhane et al. (2007) and Korendyke et al. (2006).

From 2007 December 9 – 18 *Hinode* followed NOAA active region 10978 from near disk center to the limb. During this time EIS ran a series of large ($460'' \times 384''$) slit raster studies. The exposure time at each position in the raster was 45 s and each raster ran over a period of about 5 hours. The raster was performed 9 times on this active region.

For each observation we processed the data by removing the CCD pedestal, dark current, and hot pixels. We also estimated the magnitude of the wavelength drift as a function of time. For each spectral line of interest we identified line and continuum regions and computed the line intensity, centroid, and width using moments. Finally, we account for any spatial offsets between the two CCDs by cross correlating rasters from emission lines formed at similar temperatures.

3. Emission Measure Analysis

For this initial survey of active loops observed with EIS we inspected each Fe XII 195.119 Å raster and manually identified relatively isolated portions of coronal loops. We use the spatial coordinates derived from this selection to determine the intensities in the rasters of the other emission lines. Since these loop coordinates are not necessarily aligned to the CCD we have interpolated to determine the intensities along the selected segment (see Aschwanden et al. 2008 Figure 3) and average the intensities along the loop. Examples of EIS loop segments are shown in Figures 1 and 2, where the loop is shown in various strong emission lines.

To further isolate the contribution of the loop to the observed emission we identify background pixels in Fe XII 195.119 Å and fit them with a first order polynomial. The sum over the remaining intensity between the background pixels represents the total intensity of the loop. For consistency, these same background coordinates are used to determine the background subtracted intensities in the other emission lines. To determine how co-spatial the emission at the various temperatures is, we also calculate the cross-correlation of the background subtracted intensities with Fe XII 195.119 Å. Note that we include 2 lines, Fe XII 186.880 Å and Fe XIII 203.826 Å, that form density sensitive line ratios when paired with other lines from the same ion.

The observed background subtracted line intensities are related to the differential emission measure in the usual way

$$I_\lambda = \frac{1}{4\pi} \int \epsilon_\lambda(n_e, T) \xi(T)\, dT. \tag{1}$$

Since the density is an important parameter in determining the emissivities of many of these lines, we have precomputed grids of emissivities ($\epsilon_\lambda(n_e, T)$) as a function of temperature and density with the CHIANTI atomic physics database (e.g., Landi et al. 2006) and use the density as a free parameter in the fitting. For the emission measure we consider two models, one a delta function in temperature for the isothermal approximation

$$\xi(T) = EM_0\, \delta(T - T_0), \tag{2}$$

and the other a Gaussian distribution in temperature

$$\xi(T) = \frac{EM_0}{\sigma_T \sqrt{2\pi}} \exp\left[-\frac{(T - T_0)^2}{2\sigma_T^2} \right], \tag{3}$$

which allows for a dispersion in the temperature distribution.

The calculation of the best-fit parameters for the emission measure distributions is relatively simple. The intensities for loops that are well correlated with Fe XII 195.119 Å are used directly. The averaging generally results in very small statistical errors in the intensities. In an attempt to account for additional uncertainties in the atomic data we have increased the relative errors to 20% of the observed intensities. The intensities for emission lines that are poorly correlated with Fe XII 195.119 Å ($r \leq 0.8$) are set to zero. The uncertainties in these lines are estimated to be 20% of the measured background. The intensities and uncertainties are used as inputs to a Levenberg-Marquardt algorithm for calculating the best-fit parameters.

The results of applying this analysis to 20 loop segments identified in the EIS rasters are summarized in Table 1. In almost all cases we find that the Gaussian emission measure model has a lower χ^2 than the isothermal emission measure model. The dispersion in temperature, however, is almost always narrow with $\log \sigma_T \lesssim 5.4$. This result is consistent with a visual inspection of the data which shows that these Fe XII loops are rarely evident in Si VII or Fe XV at the same time. In only two cases (loops #5 and #11) do we see emission over such a wide range of temperatures simultaneously.

For comparison with these active region loop measurements we have repeated this emission measure analysis for observations above the quiet limb, where previous work has shown the emission measure to be isothermal (e.g., Landi et al. 2002). In this case we obtain

$\log \sigma_T \simeq 5.0$ for the Gaussian DEM model and similar χ^2 values for both the Gaussian and isothermal DEM models. The results of this temperature analysis will be presented in a future paper.

The assumption of a Gaussian differential emission measure is highly restrictive. To investigate the temperature dependence of the DEM more generally we have experimented with the Markov-chain Monte Carlo (MCMC) reconstruction algorithm included in the PINTofALE spectroscopy package (e.g., Kashyap & Drake 2000). The MCMC algorithm makes no assumptions about the functional form of the DEM. The DEM computed with this method is generally consistent with the narrow DEM suggested by the Gaussian fits. In a number of cases the MCMC method suggests enhanced emission above the peak temperature in the DEM. Such a component would be consistent with the presence of cooling filaments. However, the magnitude of the high temperature component is sensitive to the errors assumed for the high temperature lines and this analysis will require additional work.

For each loop segment we have also computed the loop width from a Gaussian fit to the Fe XII 195.119 Å emission (see Table 1). Since we have also measured the density we can estimate the volume of the emitting plasma in the loop. The line of sight emission measure is simply the volume emission measure divided by the area of an EIS pixel

$$EM_0 = f\frac{n_e^2 V}{l^2} = f\frac{n_e^2 \pi r^2 l}{l^2} = f\frac{n_e^2 \pi r^2}{l}, \tag{4}$$

where r is the observed radius of the loop, l is the length of EIS pixel ($1''$), and f is the volumetric filling factor. Following Klimchuk (2000) we relate the observed loop radius to the measured width using $r = 2\sigma_w$. The filling factors derived from the Gaussian DEM parameters and Equation 4 are given in Table 1. This analysis suggests that these loops occupy only about 10% of the observed volume.

4. Discussion

Some previous work has suggested that coronal loops, as currently observed, are isothermal. For example, Aschwanden & Nightingale (2005) find that the majority of narrowest loops observed with TRACE are consistent with an isothermal DEM. Since TRACE is limited to observations in only three channels (Fe IX, Fe XII, and Fe XV) it is difficult to distinguish between an isothermal distribution and the narrow distributions that we measure spectroscopically. The general absence of Fe XV emission in the loops that we have studied is consistent with Aschwanden & Nightingale (2005). Del Zanna & Mason (2003) also found examples of relatively cool (~ 0.9 MK) nearly isothermal loops observed with low resolution spectroscopic data. These results also suggested filling factors near 1. Our filling

factor results are smaller than this, but we also find that the filling factor to be inversely proportional to the loop pressure (also see Warren et al. 2008). We do see some loops with a relatively broad emission measure distribution ($\log \sigma_T \sim 5.7$), which is consistent with the results of Schmelz et al. (2007) and Patsourakos & Klimchuk (2007). Our sample, which is small, suggests that such loops are rare, however.

These new observational results lend support to the non-equilibrium, multi-thread models of these "warm" coronal loops. It remains to be seen if hydrodynamic models can reproduce the observed loop properties. The combination of high densities and narrow temperature ranges will be difficult to reconcile with nanoflare models (e.g., Patsourakos & Klimchuk 2006). The narrow temperature distributions suggest that these filaments are evolving coherently.

The authors would like to thank Yuan-Kuen Ko for assistance with the MCMC DEM analysis. Hinode is a Japanese mission developed and launched by ISAS/JAXA, with NAOJ as domestic partner and NASA and STFC (UK) as international partners. It is operated by these agencies in co-operation with ESA and NSC (Norway). This work was supported by NASA and the Office of Naval Research/Naval Research Laboratory basic research program.

REFERENCES

Aschwanden, M. J., & Nightingale, R. W. 2005, ApJ, 633, 499

Aschwanden, M. J., Nightingale, R. W., & Alexander, D. 2000, ApJ, 541, 1059

Aschwanden, M. J., Nitta, N. V., Wuelser, J.-P., & Lemen, J. R. 2008, ApJ, 680, 1477

Cargill, P. J. 1994, ApJ, 422, 381

Culhane, J. L., et al. 2007, Sol. Phys., 60

Del Zanna, G., & Mason, H. E. 2003, A&A, 406, 1089

Kashyap, V., & Drake, J. J. 2000, BASI, 28, 475

Klimchuk, J. A. 2000, Sol. Phys., 193, 53

Korendyke, C. M., et al. 2006, Appl. Opt., 45, 8674

Landi, E., Del Zanna, G., Young, P. R., Dere, K. P., Mason, H. E., & Landini, M. 2006, ApJS, 162, 261

Landi, E., Feldman, U., & Dere, K. P. 2002, ApJ, 574, 495

Lenz, D. D., Deluca, E. E., Golub, L., Rosner, R., & Bookbinder, J. A. 1999, ApJ, 517, L155

Mok, Y., Mikić, Z., Lionello, R., & Linker, J. A. 2005, ApJ, 621, 1098

Müller, D. A. N., Peter, H., & Hansteen, V. H. 2004, A&A, 424, 289

Parker, E. N. 1983, ApJ, 264, 642

Patsourakos, S., & Klimchuk, J. A. 2006, ApJ, 647, 1452

Patsourakos, S., & Klimchuk, J. A. 2007, ApJ, 667, 591

Reale, F., & Peres, G. 2000, ApJ, 528, L45

Schmelz, J. T., Nasraoui, K., Del Zanna, G., Cirtain, J. W., DeLuca, E. E., & Mason, H. E. 2007, ApJ, 658, L119

Warren, H. P., Winebarger, A. R., & Mariska, J. T. 2003, ApJ, 593, 1174

Warren, H. P., Winebarger, A. R., Mariska, J. T., Doschek, G. A., & Hara, H. 2008, ApJ, 677, 1395

Winebarger, A. R., Warren, H. P., & Mariska, J. T. 2003, ApJ, 587, 439

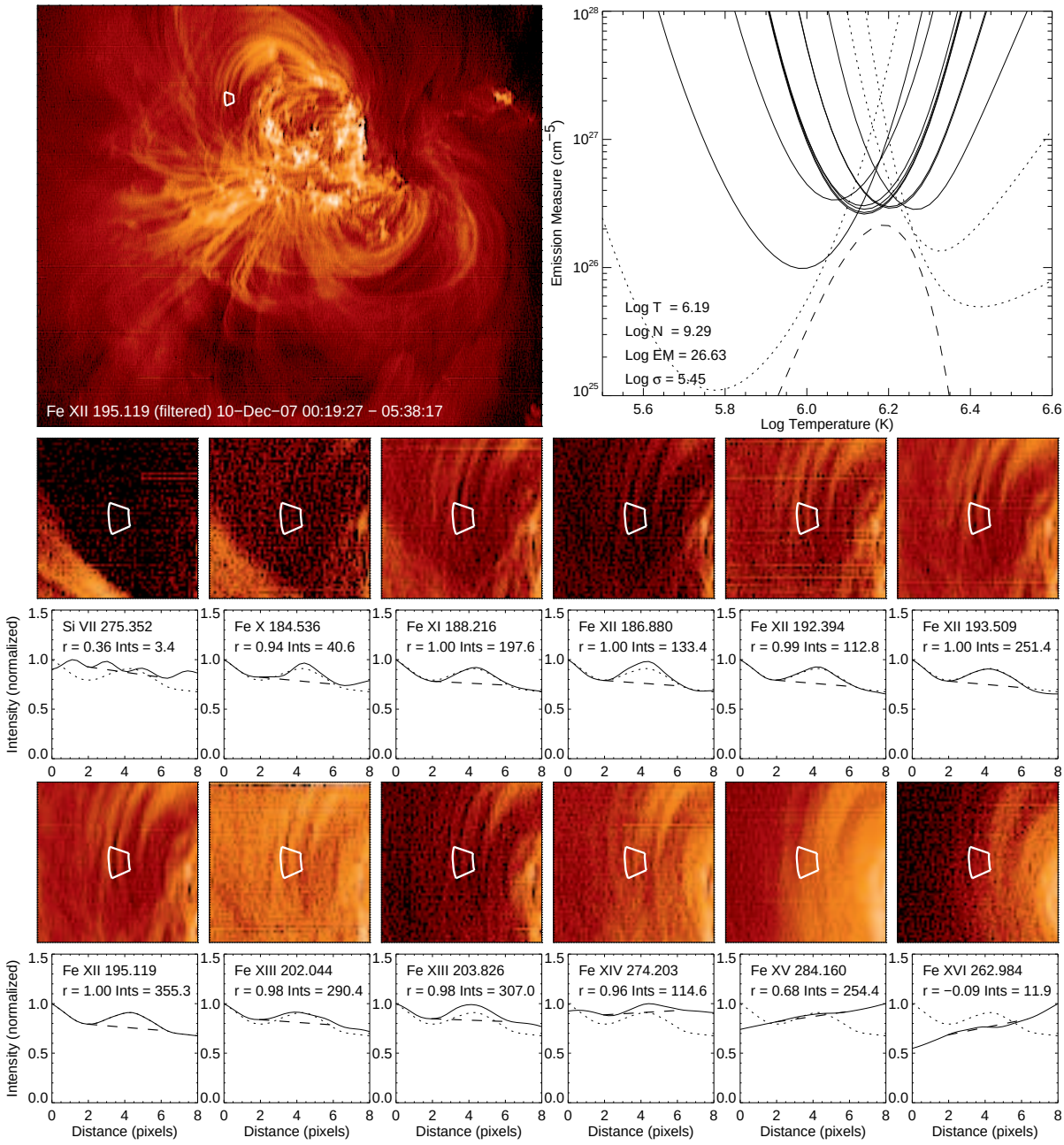

Fig. 1.— The emission measure analysis of a coronal loop segment observed with EIS. The region of interest is indicated with the white lines. The intensities averaged along the loop segment are also shown. For comparison the Fe XII 195.119 Å intensities are repeated in each plot with the dotted line. The background is indicated with the dashed line. The upper right panel shows the EM loci for each line as well as the computed emission measure distribution. The dotted EM loci curves indicate that the intensities for these lines are not well correlated with Fe XII 195.119 Å. The correlation (r) between the intensity in the displayed loop intensity and the loop intensity in Fe XII 195.119 Å is given in the legend. The displayed images have been filtered to emphasize the contrast between the loops and the background emission. This is loop # 1 in Table 1.

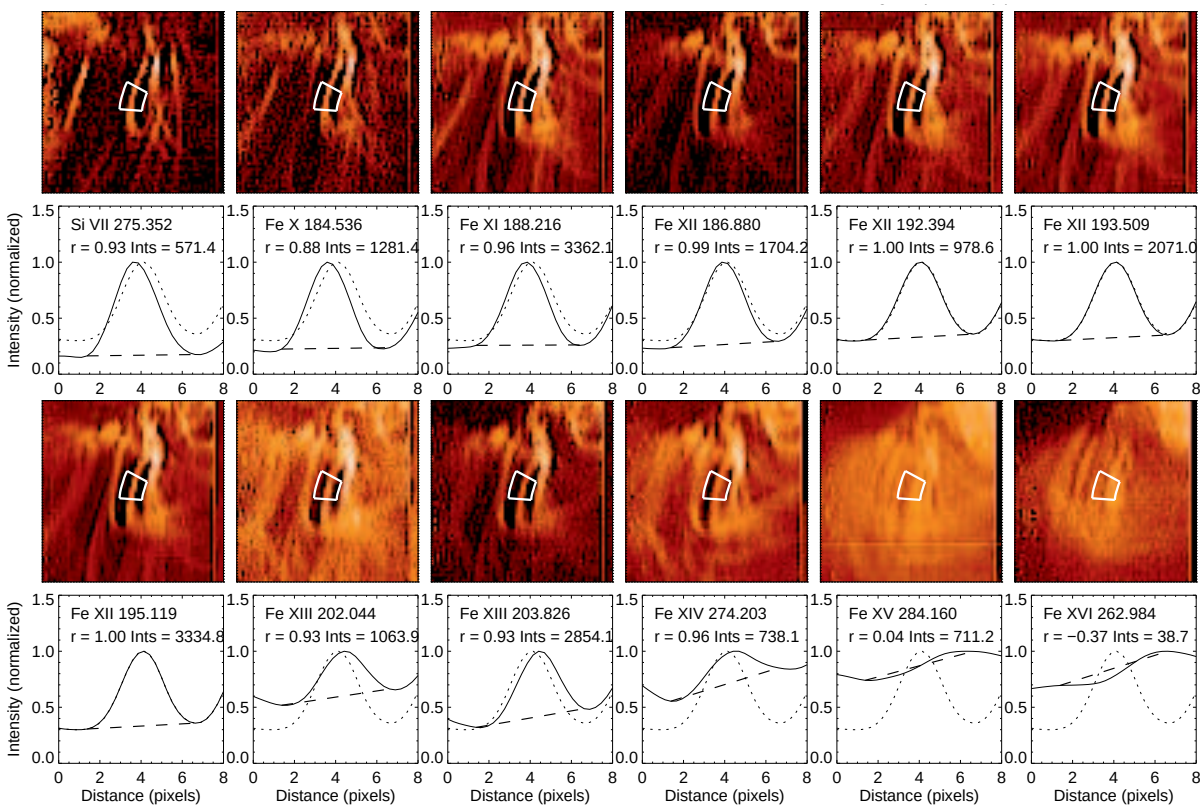

Fig. 2.— A loop segment observed with EIS on 2007 December 12. The display is similar to what is shown in Figure 1. This loop, however, appears over a broader range of temperatures. The field of view shown in $64'' \times 64''$. This is loop # 5 in Table 1.

Table 1. Emission Measure Analysis of Active Region Loops Observed with EIS[a]

					Isothermal			Gaussian						
#	Date	t_{start}	t_{end}	σ_w	EM_0	n_0	T_0	EM_0	n_0	T_0	σ_T	χ^2_I	χ^2_G	$f(\%)$
1	10-Dec-07	03:36:43	03:37:25	1.18	26.52	9.25	6.16	26.63	9.29	6.19	5.45	1.71	0.79	9.1
2	11-Dec-07	13:11:02	13:11:43	1.42	27.18	9.77	6.11	27.28	9.86	6.15	5.44	2.13	0.88	2.0
3	11-Dec-07	12:57:50	13:01:18	1.35	26.90	9.56	6.13	27.06	9.66	6.16	5.55	2.86	1.44	3.3
4	12-Dec-07	06:31:29	06:36:21	1.36	26.72	9.58	6.06	26.79	9.57	6.07	5.44	2.14	1.49	2.6
5	12-Dec-07	06:29:24	06:30:47	0.97	27.66	9.61	6.07	27.90	9.84	6.01	5.70	5.49	1.52	19.6
6	12-Dec-07	14:52:33	14:53:56	1.17	27.25	9.28	6.07	27.34	9.43	6.08	5.54	4.68	1.49	24.2
7	12-Dec-07	15:01:34	15:07:08	1.54	26.62	9.20	6.08	26.64	9.24	6.08	5.18	1.42	1.31	6.8
8	13-Dec-07	15:35:17	15:36:41	1.19	27.47	9.71	6.20	27.49	9.65	6.20	5.28	1.69	1.58	12.0
9	13-Dec-07	13:45:32	13:46:55	0.97	26.68	9.34	6.16	26.83	9.32	6.12	5.45	3.91	1.65	18.4
10	15-Dec-07	03:40:08	03:41:31	1.03	26.44	9.29	6.12	26.45	9.31	6.12	4.99	0.79	0.85	7.0
11	15-Dec-07	01:44:07	01:44:49	1.20	26.64	9.50	6.13	26.80	9.62	6.20	5.62	3.73	3.59	2.8
12	15-Dec-07	21:17:07	21:23:22	2.30	26.72	9.27	6.17	26.77	9.27	6.16	5.31	2.69	1.48	3.5
13	15-Dec-07	19:50:59	19:52:22	1.69	26.17	9.39	6.16	26.35	9.41	6.16	5.55	1.46	0.85	1.3
14	18-Dec-07	02:15:51	02:17:14	1.07	27.53	10.98	6.19	27.55	10.50	6.18	5.44	2.98	1.52	0.3
15	18-Dec-07	01:11:14	01:14:43	1.57	26.51	9.15	6.19	26.68	9.13	6.16	5.55	3.16	1.66	11.5
16	18-Dec-07	01:39:43	01:44:35	2.73	27.05	9.43	6.15	27.14	9.50	6.17	5.42	1.85	1.12	2.1
17	18-Dec-07	19:51:37	19:55:05	1.16	26.75	9.86	6.20	26.84	9.76	6.17	5.52	1.86	1.34	1.7
18	10-Dec-07	03:27:00	03:32:33	1.28	26.89	9.39	6.22	26.92	9.34	6.21	5.36	1.36	1.18	11.6
19	11-Dec-07	13:13:48	13:15:53	0.90	26.60	9.99	6.19	26.69	10.02	6.20	5.40	1.00	0.42	0.6
20	13-Dec-07	16:08:38	16:10:01	1.04	26.49	9.47	6.10	26.58	9.51	6.09	5.33	2.13	1.20	3.7

[a]The date and times given indicate when EIS was rastering over the loop segment. The paramter σ_w is the loop width in pixels measured in Fe XII 195.119 Å. The base-10 logarithm of the emission measure parameters are given.